Mathematical modeling of a V-stack piezoelectric aileron actuation

Ioan URSU*[,1], Dragos Daniel ION GUTA[1], Daniela ENCIU[1],
Adrian TOADER[1], Mircea DAN[1], Cristiana DONCIU[1],
Vasile TURCAN[1]

*Corresponding author
[1]INCAS – National Institute for Aerospace Research "Elie Carafoli",
B-dul Iuliu Maniu 220, Bucharest 061126, Romania,
ursu.ioan@incas.ro*, guta.dragos@incas.ro, enciu.daniela@incas.ro,
toader.adrian@incas.ro, dan.mircea@incas.ro, donciu.cristina@incas.ro

Abstract: The article presents a mathematical modeling of aileron actuation that uses piezo V-shaped stacks. The aim of the actuation is the increasing of flutter speed in the context of a control law, in order to widen the flight envelope. In this way main advantage of such a piezo actuator, the bandwidth is exploited. The mathematical model is obtained based on free body diagrams, and the numerical simulations allow a preliminary sizing of the actuator.

1. INTRODUCTION

Aeroelasticity is the discipline that studies the interaction of inertial, structural and aerodynamic forces on aircraft, buildings, surface vehicles, etc. The interaction between these three forces can cause several undesirable phenomena: divergence (static aeroelastic phenomenon); flutter (dynamic aeroelastic phenomenon); limit cycle oscillations (nonlinear aeroelastic phenomenon); vortex shedding, buffeting, galloping (unsteady aerodynamic phenomena). There is a fairly clear description of "aeroelastic flutter" on Wikipedia: "Flutter is a self-feeding and potentially destructive vibration where aerodynamic forces on an object couple with a structure's natural mode of vibration to produce rapid periodic motion". In principle, the variation of eigenvalues of a structural model, driven by aerodynamic flow variation is studied in the linear frame. The flow variation causes the change of the aerodynamic forces that are proportional to the flow velocity of air and degrees of freedom of the system; in turn, this influences the aeroelastic system, thereby modifying their eigenvalues until they become "unstable". Flutter occurs when the air speed reaches a speed called the *flutter speed.*

The countering of dangerous phenomena such as flutter and buffeting, for example, was made first by passive techniques: increasing structural rigidity, mass balancing, changing geometry. This led to increase both weight and cost, while reducing overall performance. At some point, the use of primary flight controls and associated actuators was considered efficient to

combat flutter [1]-[4]. Thus began the active control era [5]. However, as demonstrated in [6], there are many drawbacks when using primary flight controls for auxiliary purposes.

The purpose of this paper is to present a solution to counteract the flutter, based on the use of an actuator consisting in two V-shaped piezo stacks (Fig. 1.). The approach is developing in the project [8] and ends as a demonstrator in wind tunnel.

The advantage of the piezo actuators is their small size, large bandwidth and, not least, high energy density. There is a disadvantage linked to their lower strokes. It is important to note that, for the antiflutter aero-elastic control to be effective, the deflection of the control surface must be at least 5-6 degrees, to the frequency range of at least 25 to 30 Hz, as states the paper [9]. The piezo stacks NAC2022-H98-AO1 were bought from NOLIAC (http://www.noliac.com/) and have the following basic properties: height 98 mm, stroke 148.8 μm, capacitance 19010 nF, maximal force developed 4200 N, maximum operating temperature 150°C, material NCE51F.
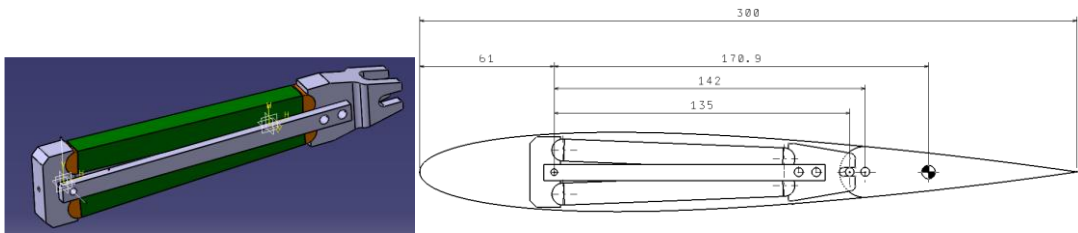
Fig. 1. Left: CATIA 3D view of the V-shaped piezo stacks; right: framing of actuator in the available space in wing
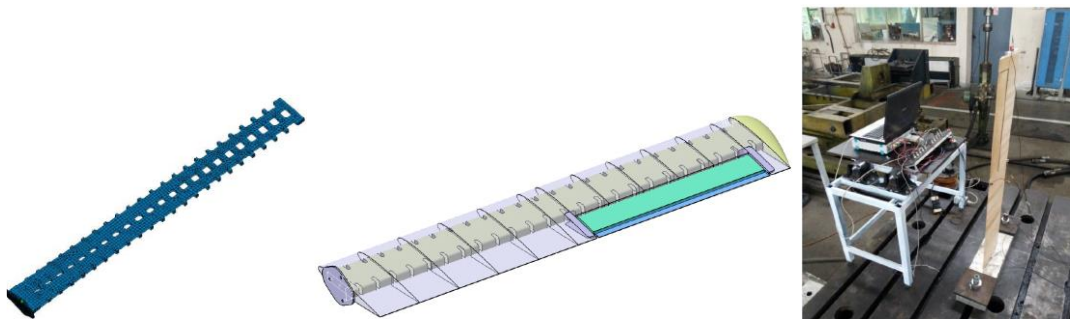
Fig. 2. CATIA model of the longeron (top left) and wing (top middle); measuring of wing model frequencies (top right) [7]

Table 1. Natural frequencies, determined by CATIA, and measured, respectively

Mode number	Frequency Hz (longeron) CATIA computed	Frequency Hz (wing) CATIA computed	Frequency Hz (wing) measured
1	13.59	6.23	5.93 bending
2	43.42	10.21	11.70 torsion
3	44.12	20.83	22.73 bending
4	59.14	26.32	
5	78.91	29.83	

The actuator is mounted inside the wing, to the far right of the aileron visible in Fig. 2. top middle. The same figure presents a CATIA drawing of the longeron and the experimental facility for measuring natural frequencies of the wing model. Table 1 shows natural frequencies, CATIA computed and measured. In general, the frequency of flutter occurs in

the domain of the first two frequencies of the wing, thus the bandwidth of the actuator has to well cover this frequency range.

2. KINEMATIC SCHEME OF AILERON ACTUATION WITH TWO V SHAPED -STACK PIEZOELECTRIC ACTUATORS

The scheme is represented in Fig. 3. *The xOy* system of axes, with the Ox axis along the axis is considered. The coordinates are expressed in [mm]. *We mention that the left side of the scheme is actually in a different parallel plane to the right side, the one in which the aileron and the slider crank mechanism, sketched in the point* P_6, *are represented.*

According to the conception and the rigors of actuation with such actuators, the piezo stacks are arranged along the segments P_1P_3 and P_2P_4, respectively. When the stack P_1P_3 is activated by increasing supply voltage V, $V_{01} + \Delta V(t-\tau)$, which determines its extension to move to the right and slightly below the articulated point P_3, the stack P_2P_4 is supplied with the voltage $V_{02} - \Delta V(t)$

$$\Delta V(t-\tau) = \begin{cases} 0, t \leq \tau \\ \Delta V, t > \tau \end{cases}$$

which causes the withdrawal to the left and slightly upward of the articulated point P_4, therefore to not oppose resistance to movement down of the articulated point P_5 in the slider crank mechanism. This provides the movement with positive angle (up) δ of the aileron. The two stacks are successively active versus passive, in the sense of the presented description. The constant τ defines a delay in the application of voltage to "active" stack, to ensure the withdrawal of passive stack.
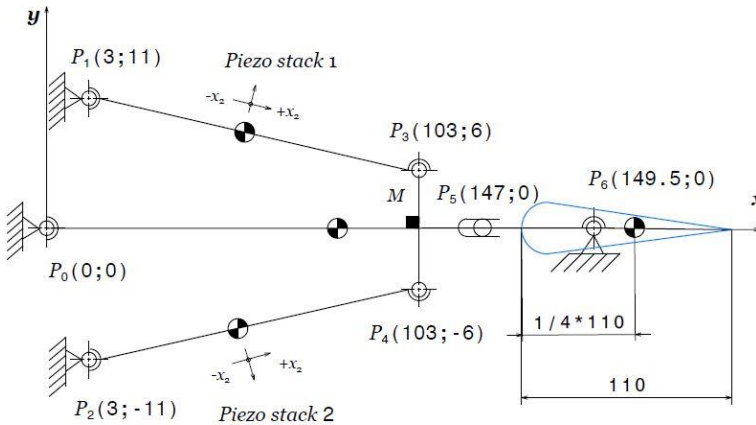
Fig. 3. Kinematic scheme of aileron actuation with 2 V-shaped piezo stacks; coordinates in mm

The calculation of the aileron deflection, assuming to neglect the elasticities, the friction and the aerodynamic load on aileron, takes into account the following reasons:
a) simplifying hypothesis: because only one stack is active, consider that the physical model of the actuation is that of Fig. 4, which represents the sequence of the aileron up deflection by activating the piezo stack placed on the segment;
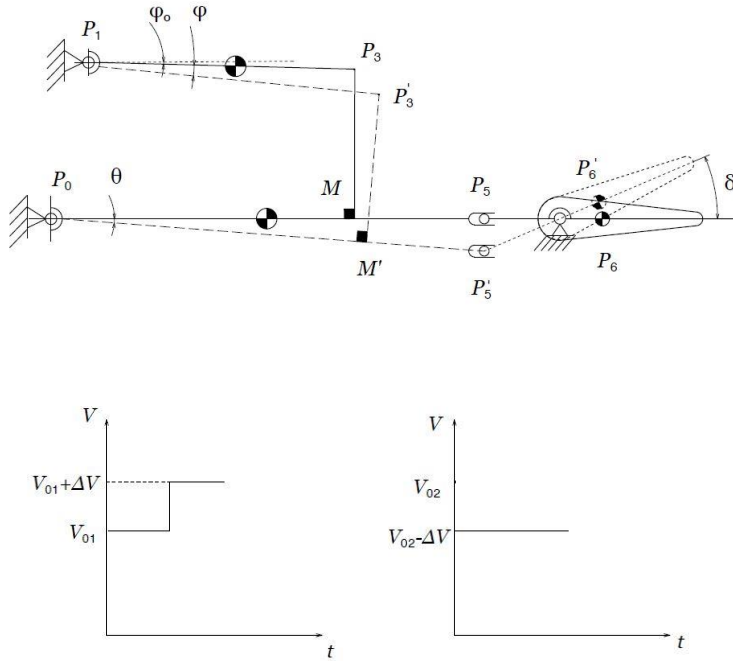
Fig. 4. Above: A simple physical model of aileron actuation; below: the form of voltage signals at the inputs of the two piezo stacks, in a time sequence

b) the lever P_1P_3 is articulated with the lever P_3M, the lever P_3M is solidary linked with the shaft P_0P_5, and in the point P_5 there is a slider crank type joint for aileron actuation;

c) in the presence of the control voltage V, the piezo stack P_1P_3 develops an expansion movement, and the piezo stack P_2P_4 develops a movement of withdrawal, if it has previously been extended, and, based on constraints, the point P_3 moves on an arc in the point P_3', the lever $P_3'M'$ remaining solidary, without deformations, with P_0M'.

3. THE PIEZO STACK FREE STROKE AND THE AILERON DEFLECTION DETERMINATION WITH RESPECT TO THE APPLIED VOLTAGE

In what follows, we propose a mathematical model of the aileron actuation, with no load at the output of the actuator. Referring to Fig. 4., the angle δ will be obtained as a function of the control voltage V applied to the piezo stack disposed on the shaft P_1P_3. As a result of the applied voltage, considering the articulation in the point P_3, and the assumption that the length of the segments P_0M and P_3M solidary connected at an angle of 90 degrees, remains constant, the point P_3 moves in P_3' and the point M moves in M'.

The following design data are considered

$$x_{P_3} = 103\,\text{mm}; \ y_{P_3} = 6\,\text{mm}; \ x_{P_1} = 3\,\text{mm}; \ y_{P_1} = 11\,\text{mm}; \ x_{P_5} = 147\,\text{mm}; \ x_M = 103\,\text{mm}$$

$$L_1 = P_1P_3 = \sqrt{\left(x_{P_3} - x_{P_1}\right)^2 + \left(y_{P_3} - y_{P_1}\right)^2}; \ L_2 = MP_0 = M'P_0$$

$$L_3 = M'P_3' = MP_3 = y_{P_3}; \ L_4 = P_0P_5 = x_{P_5}$$

The length of segment P_0M' is

$$x_{M'}^2 + y_{M'}^2 = L_2^2 \tag{1}$$

Now, we transcribe the squareness condition $P_3'M' \perp P_0M'$

$$\frac{y_{M'}}{x_{M'}} \cdot \frac{y_{P_3'} - y_{M'}}{x_{P_3'} - x_{M'}} = -1, \ \ y_{M'}y_{P_3'} + x_{M'}x_{P_3'} - \left(x_{M'}^2 + y_{M'}^2\right) = 0$$

or, considering the relationship (1)

$$y_{M'}y_{P_3'} + x_{M'}x_{P_3'} = L_2^2 \tag{2}$$

The free stroke of piezostack at the point P_3, is approximated with a line passing through the origin (Fig. 5) and having the slope

$$k = \frac{147}{200}\frac{10^{-6}m}{V} = 0.735 \times 10^{-3}\frac{mm}{V} \tag{2'}$$

Therefore, the length of the segment P_1P_3' is

$$\left(x_{P_3'} - x_{P_1}\right)^2 + \left(y_{P_3'} - y_{P_1}\right)^2 = \left(L_1 + kV\right)^2 \tag{3}$$

and the length of the segment $P_3'M'$ is

$$\left(x_{M'} - x_{P_3'}\right)^2 + \left(y_{M'} - y_{P_3'}\right)^2 = L_3^2 \tag{4}$$

We have to solve a system of four equations (1)-(4) with four unknowns $x_{P_3'}, \ y_{P_3'}, \ x_{M'}, \ y_{M'}$.

Determining the coordinates of P_3'

By developing (4) and using (1) and (2) one obtains

$$x_{P_3'}^2 + y_{P_3'}^2 = L_3^2 + L_2^2 \tag{5}$$

From (3) one obtains

$$x_{P_3'}x_{P_1} + y_{P_3'}y_{P_1} = E(V) := \frac{1}{2}\left[x_{P_1}^2 + y_{P_1}^2 + L_2^2 + L_3^2 - \left(L_1 + kV\right)^2\right] \tag{6}$$

With the notations

$$A = x_{P_1}^2 + y_{P_1}^2, B = -2E(V)x_{P_1}, C = -y_{P_1}^2\left(L_2^2 + L_3^2\right) + E^2(V) \tag{7}$$

we determine the coordinates of point P_3'

$$x_{P_3'} = \frac{-B + \sqrt{B^2 - 4AC}}{2A}, \ y_{P_3'} = \sqrt{L_2^2 + L_3^2 - x_{P_3'}^2} \tag{8}$$

Determining the coordinates of M'

$$\begin{cases} x_{M'}^2 + y_{M'}^2 = L_2^2 & \Rightarrow \ \ y_{M'} = \sqrt{L_2^2 - x_{M'}^2} \tag{9_1} \\ x_{M'}x_{P_3'} + y_{M'}y_{P_3'} = L_2^2 \end{cases}$$
$$\tag{9_2}$$

The expression of $y_{M'}$ from (9_1) is substituted in (9_2)

No°	Increasing voltage [V]	Displacement [μm]	Decreasing voltage [V]	Displacement [μm]
1	10	6	200	147
2	30	21	180	139
3	60	44	150	126
4	90	68	120	109
5	120	92	90	89
6	150	114	60	66
7	180	135	30	38
8	200	146	10	15
9			MUTE(0)	6

piezo stacks measurements: 1 above, 2 below

No°	Increasing voltage [V]	Displacement [μm]	Decreasing voltage [V]	Displacement [μm]
1	10	5	200	154
2	30	19	180	146
3	60	44	150	132
4	90	69	120	115
5	120	95	90	94
6	150	117	60	71
7	180	139	30	43
8	200	153	10	20
9			MUTE(0)	8
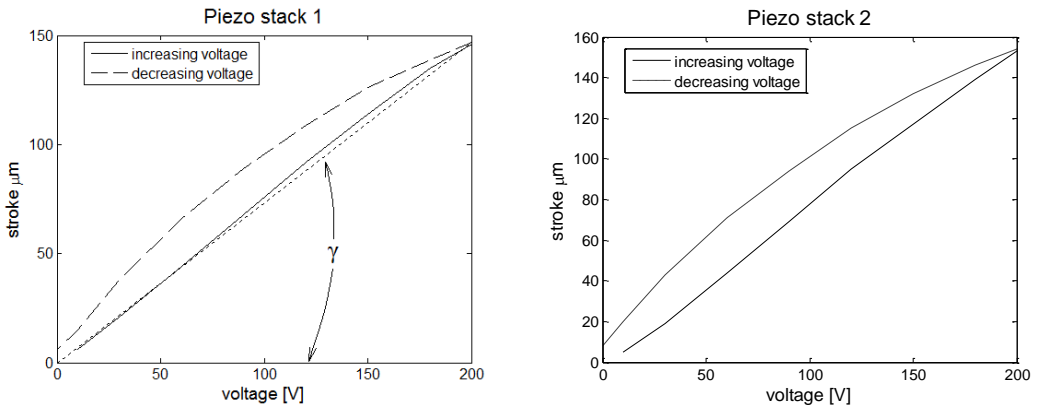
Fig. 5. Free stroke measurements for piezo stacks; $k := \operatorname{tg}(\gamma)$

$$x_{M'} x_{P_3'} + y_{P_3'} \sqrt{L_2^2 - x_{M'}^2} = L_2^2, \quad y_{P_3'} \sqrt{L_2^2 - x_{M'}^2} = L_2^2 - x_{M'} x_{P_3'}$$

$$y_{P_3'}^2 \left(L_2^2 - x_{M'}^2\right) = L_2^4 + x_{P_3'}^2 x_{M'}^2 - 2L_2^2 x_{M'} x_{P_3'}, x_{M'}^2 x_{P_3'}^2 - 2L_2^2 x_{M'} x_{P_3'} + x_{M'}^2 y_{P_3'}^2 + L_2^4 - L_2^2 y_{P_3'}^2 = 0 \qquad (10)$$

$$x_{M'}^2 \left(x_{P_3'}^2 + y_{P_3'}^2\right) - 2L_2^2 x_{P_3'} x_{M'} + L_2^2 \left(L_2^2 - y_{P_3'}^2\right) = 0$$

Thus the coordinates of point M' are the following

$$x_{M'} = \frac{-B + \sqrt{B'^2 - 4A'C'}}{2A'}, \, y_{M'} = \sqrt{L_2^2 - x_{M'}^2} \tag{11}$$

$$A' := x_{P_3'}^2 + y_{P_3'}^2, B' := -2L_2^2 x_{P_3'}, C' := L_2^2 \left(L_2^2 - y_{P_3'}^2 \right)$$
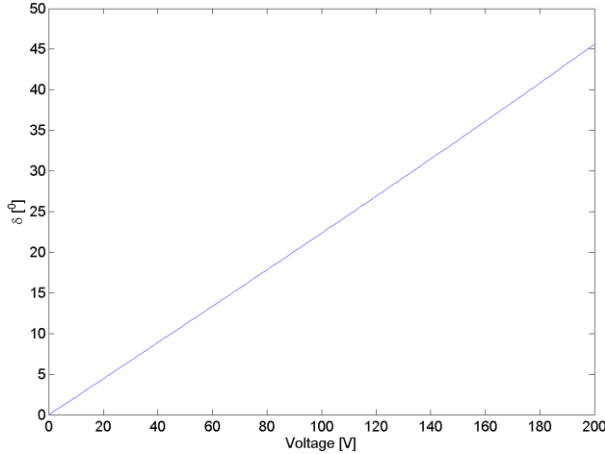
Fig. 6. Evolution of the aileron deflection angle δ (Fig. 4.) with respect to the voltage V

Determining the angle δ

Consider triangles $P_o MM'$, $P_o P_5 P_5'$, Fig. 4 above, as similar, thus Thales theorem gives

$$\frac{P_0 M}{P_0 P_5} = \frac{MM'}{P_5 P_5'}, \frac{L_2}{L_4} = \frac{MM'}{P_5 P_5'} \tag{12}$$

$$P_5 P_5' = \frac{L_4 \times MM'}{L_2} \tag{13}$$

$$MM' = \sqrt{\left(x_{M'} - x_M \right)^2 + \left(y_{M'} - y_M \right)^2} \tag{14}$$

Finally, let us assimilate the triangle $P_5 P_5' P_6$ as isosceles, then

$$\sin\left(\frac{\delta}{2}\right) = \frac{P_5 P_5'}{2 P_5 P_6}, \, P_5 P_6 = 2.5\,\text{mm} \tag{15}$$

Therefore

$$\delta = 2 \arcsin \frac{P_5 P_5'}{2 P_5 P_6} \tag{16}$$

Evolution of angle δ depending on the voltage V is given in Fig. 6.

4. COMPUTING THE ACTUATION IN THE PRESENCE OF AERODYNAMIC LOAD

We consider the actuation in the presence of the aerodynamic load on the wing, but with the neglecting of the elasticities and the frictions in the kinematic linkages. The physical model of Fig. 2 is split into 3 "bodies" (Figs. 7, 8). To obtain the actuation mathematical model, the equations of forces and moments will be written using the so-called "free body diagrams". Most notations are deductible from Figures.

The sense of Ox, Oy axes is given in Fig. 3. When the sense of the forces is evident, it will be used as such in equations. Otherwise, the sense of the reactions in supports will result algebraically:

$$m_a \ddot{x}_a = H_1 + F_3 \cos\varphi - F_3' \sin\varphi$$
$$m_a \ddot{y}_a = V_1 - F_3 \sin\varphi - F_3' \cos\varphi \tag{17}$$
$$J_0 \ddot{\varphi} = m_a g \, l_{ag} \cos\varphi + F_3' l_a$$

$$m_s \ddot{x}_{cg} = H_0 - F_3 \cos\varphi + F_3' \sin\varphi - F_5 \sin\theta$$
$$m_s \ddot{y}_{cg} = V_0 - m_s g + F_3 \sin\varphi + F_3' \cos\varphi - F_5 \cos\theta \tag{18}$$
$$J_s \ddot{\theta} = m_s g \, l_{scg} \cos\theta - F_3 \sin\varphi \, d_{31} - F_3' \cos\varphi \, d_{32} + F_5 D \cos\theta$$

$$m_e \ddot{x}_{cg} = -F_5 \sin\theta + H_6 - F_a \sin\delta$$
$$m_e \ddot{y}_{cg} = F_5 \cos\theta + V_6 - F_a \cos\delta - m_e g \tag{19}$$
$$J_e \ddot{\theta} = l_e F_5 \cos\theta - M_a - m_e g \, l_g$$
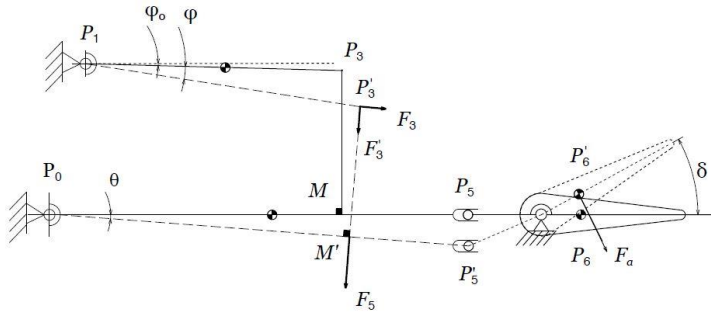
Fig. 7. Scheme for computing the actuation and introducing the method of "free body diagrams"

Determination of the actuation evolution means the solving of the system of 9 equations (17), (18), (19) with 9 unknowns $H_0, V_0, F_3, F_3', F_5, H_1, V_1, H_6, V_6$. Input data are the following: $l_a = 100.12$mm $\cong \overline{P_1 P_3}$; $l_e \cong \overline{P_5' P_6} \cong = 2.5$mm; $l_g = P_6 P_7 = 15.77$mm; $l_{ag} = 100.12/2$ mm; $m_a = 0.079$kg; $m_s = 0.071$kg; $d_{32} = 103$mm; $D = 147$mm; $l_{scg} = 90$mm; $m_e = 0.12$kg; $S_e = 0.11 \times 0.49$m^2; $c_e = 110$mm; $\rho = 1.3$kg/m^3; $U = 0 \ldots 50$m/s; $M_a = 0.5\rho U^2 S_e c_e C$ [Nm]; $C = 0.01 \ldots 0.1$; $F_a = 4M_a/c_e$ [N]. The segments $l_a, l_e, l_g, l_{ag}, d_{32}, D, l_{scg}$ involved in the moments calculation were considered to be constant. Other approximations are inherent.
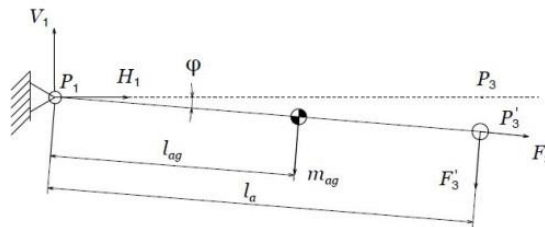
Fig. 8a. The body of piezo stack
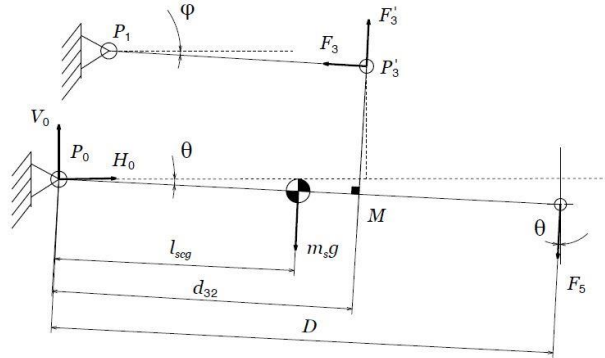
Fig. 8b. The body of the central lever
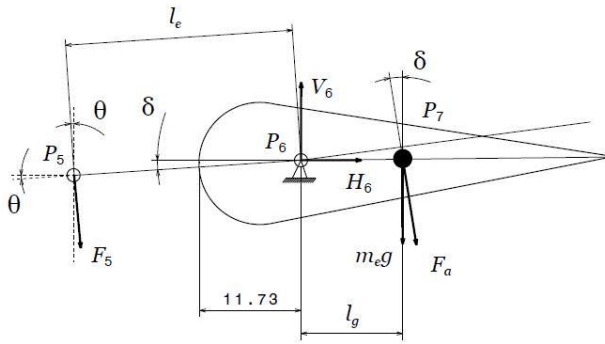
Fig. 8c. The body of the actuation, downstream of slider crank

$$F_5 \times P_5'P_6 = F_a \times l_g \qquad (20)$$

Measurements of the displacement-force at the level of point P_5 were performed (Fig. 10). The displacement of 650 μm corresponds to a half of sinusoid without load. The double, 1300 μm, i.e., 1.3mm, is an increase of approximate 10 times of the piezo stack stroke given by the provider (148.8μm; see http://www.mmech.com/noliac-actuators/plate-stacks/nac2022-hxx). The developed maximum force, as measured by loading with resorts becoming increasingly stronger on the other half of the sinusoid, is 230 N. Thus, on the shaft P_1P_3 the force of 4600N (close to 4200N given by the provider) is checked. In this theoretical-experimental framework, we have to adapt equation (3) to the new situation in which the piezo stack stroke will be affected by aerodynamic load F_a. Our reasoning is as follows. At the hinge axis represented by the fulcrum P_6, we have the balance of moments. Add the simplifying assumption of equilibrium of moments at the points P_3, P_5

$$4600 \times x\,[\text{Nm}] = 1.3 \times 10^{-3} \times F_5\,[\text{Nm}] \qquad (20')$$

Combining the two relationships above, the sought correction of the piezo stack stroke is

$$x\,[\text{m}] = \frac{1.3 \times 10^{-3}\,[\text{m}] \times l_g}{4600\,[\text{N}] \times l_e} F_a\,[\text{N}] \qquad (20'')$$

$$l_g = 0.25 \times 0.11 - 0.01173\,[\text{m}] = 0.01577\,[\text{m}], l_e = 2.5 \times 10^{-3}\,[\text{m}]$$

The evolution of the piezo stack stroke due to application of input voltage V is given by

$$\left(x_{P_3'} - x_{P_1}\right)^2 + \left(y_{P_3'} - y_{P_1}\right)^2 = \left(L_1 + kV - lF_a\right)^2, k = 0.735 \times 10^{-6} \frac{m}{V}$$

$$l := \frac{1.3 \times 10^{-3} \times l_g}{4600 \times l_e} = 1.7827 \times 10^{-6} \frac{m}{N}, M_a = 0.5 \times \rho U^2 S c_e C \tag{3'}$$

$$F_a = 4 \times M_a / c_e, c_e = 0.11 \text{ m}, S = 0.11 \times 0.49 \text{ m}^2, U = 0...50 \text{ m/s}, C = 0.01...0.1$$

Therefore, the algorithm for calculating the actuation in the presence of the aerodynamic load F_a requires solving a system of 9 equations with 9 unknowns $H_0, V_0, F_3, F_3', F_5, H_1, V_1, H_6, V_6$, for a set V_i of values in the range $(100; 200)$ V and a set U_i of values in the range (0 ... 50) m/s.

$$H_1 + F_3 \cos\varphi - F_3' \sin\varphi = 0, V_1 - F_3 \sin\varphi - F_3' \cos\varphi = 0$$

$$m_a g l_{ag} \cos\varphi + F_3' l_a = 0, H_0 - F_3 \cos\varphi + F_3' \sin\varphi - F_5 \sin\theta = 0$$

$$V_0 - m_s g + F_3 \sin\varphi + F_3' \cos\varphi - F_5 \cos\theta = 0$$

$$m_s g l_{scg} \cos\theta - F_3 \sin\varphi d_{31} - F_3' \cos\varphi d_{32} + F_5 D \cos\theta = 0 \tag{21}$$

$$-F_5 \sin\theta + H_6 + F_a \sin\delta = 0, F_5 \cos\theta + V_6 - F_a \cos\delta - m_e g = 0$$

$$l_e F_5 \cos\theta - M_a - m_e g l_g = 0$$

The notations in (3') that do not appear in the Figures refer to aerodynamic moment M_a, coefficient of aerodynamic moment C, air speed U, air density ρ, aileron surface S, aerodynamic chord c_e of aileron.

The point of application of the aerodynamic force is considered at a quarter of chord versus the leading edge.

Obviously, the solutions will represent stationary regimes that V-piezo stacks actuation can achieve as responses to voltage command signals. The angle values θ and φ are calculated with the same relationships as in the case with no load. The relation (6) is restructured in the form

$$E(V; F_a) := \frac{1}{2}\left[x_{P_1}^2 + y_{P_1}^2 + L_2^2 + L_3^2 - \left(L_1 + kV - lF_a\right)^2 \right] \tag{6'}$$
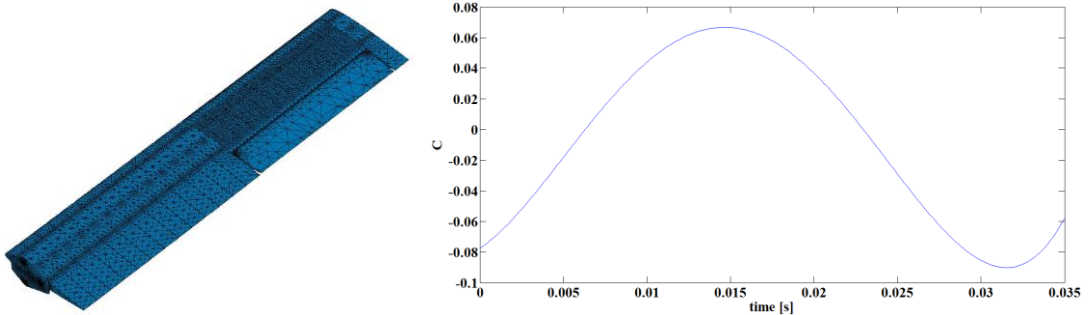
Fig. 9. Left: CATIA wing and aileron view; right: typical variation of coefficient C
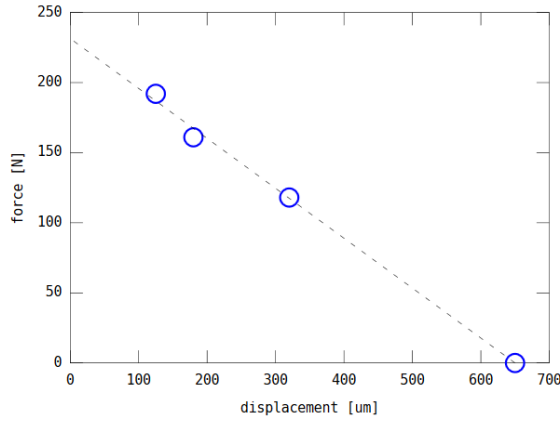
Fig. 10. Experimental measurements displacement-force, at the level of point P_5 (see Fig. 3)
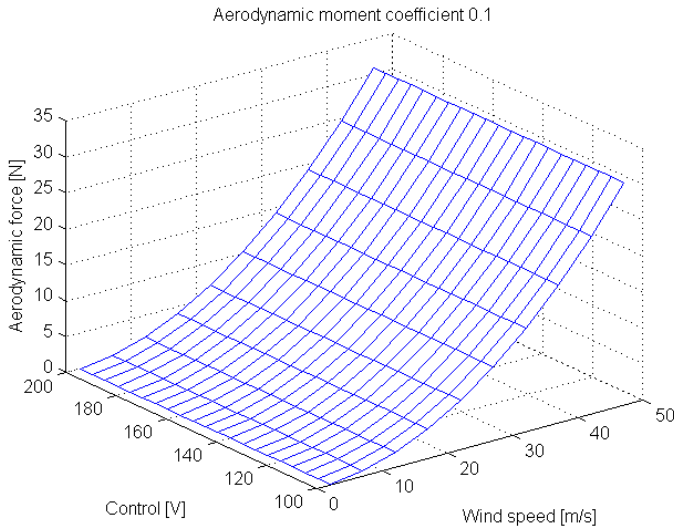
Fig. 11. Stationary values of aerodynamic force F_a, depending on air speed U

Therefore, the algorithm has the following sequences
  − the coordinates of the point P_3' (see (8))

$$x_{P_3'} = \frac{-B + \sqrt{B^2 - 4AC}}{2A}, \, y_{P_3'} = \sqrt{L_2^2 + L_3^2 - x_{P_3'}^2}$$

$$A := x_{P_1}^2 + y_{P_1}^2, B := -2E(V, F_a) x_{P_1}, C := -y_{P_1}^2 \left(L_2^2 + L_3^2 \right) + E^2(V, F_a) \tag{22}$$

  − the coordinates of the point M' (see (10))

$$x_{M'} = \frac{-B + \sqrt{B'^2 - 4A'C'}}{2A'}, \, y_{M'} = \sqrt{L_2^2 - x_{M'}^2}$$

$$A' := x_{P_3'}^2 + y_{P_3'}^2, B' := -2L_2^2 x_{P_3'}, C' := L_2^2 \left(L_2^2 - y_{P_3'}^2 \right) \tag{23}$$

  − the trigonometric functions values for angle θ, φ and the values of angle δ

$$\sin\theta = \frac{|y_{M'}|}{\sqrt{x_{M'}^2 + y_{M'}^2}}, \quad \cos\theta = \sqrt{1 - \sin^2\theta}$$

$$\sin\varphi = \frac{|y_{P_3'} - y_{P_3}|}{\sqrt{\left(x_{P_3'} - x_{P_1}\right)^2 + \left(y_{P_3'} - y_{P_1}\right)^2}}, \quad \cos\varphi = \sqrt{1 - \sin^2\varphi} \tag{24}$$

$$\delta = 2\arcsin\frac{P_5 P_5'}{2 P_5 P_6}, P_5 P_5' = \frac{L_4 \times MM'}{L_2}, L_2 := \sqrt{y_{M'} y_{P_3'} + x_{M'} x_{P_3'}}, L_4 := P_0 P_5 = x_{P_5}$$

In all calculation sequences must be fulfilled the condition

$$k V_i - l F_{a,j} > 0 \tag{25}$$

5. NUMERICAL SOLUTIONS AND CONCLUSIONS

Let's remind that the solutions $H_0, V_0, F_3, F_3', F_5, H_1, V_1, H_6, V_6$ of the system (21) depend on the command voltage V and the air speed U. For reasons of printing space, only six of the nine solutions, most representative for the idea of global solving are considered in Figures 5.1-5.6; the solutions are shown in the form of meshes. The maximal moment coefficient $C = 0.1$ was considered as covering from viewpoint of emphasizing the maximum forces occurring in the kinematic chain. Fig. 11 shows the order of magnitude of aerodynamic force, in other words, of the load to be acted successively by piezo stacks, in a sense or another of the movement. The reference values of the coefficient C represented in Fig. 9 was provided by Aerodynamics Compartment in the framework of the project internal reports [7]. The notation "control [V]" refers to an open loop command voltage. As shown in Fig. 12, the aerodynamic forces seem to load at a low level the piezo actuator (approximate at one eighth of the maximum force available). Figure 13 shows another important result of modeling, i.e, the angle of deflection values. Compared to values in Fig. 14, they are easily diminished, which is natural given the consideration of aerodynamic force. Figures 14 and 15 show that the reactions in supports are reasonable. Finally, Fig. 16 shows that the calculated force F_5 is quite close to the measured values (Fig. 10).
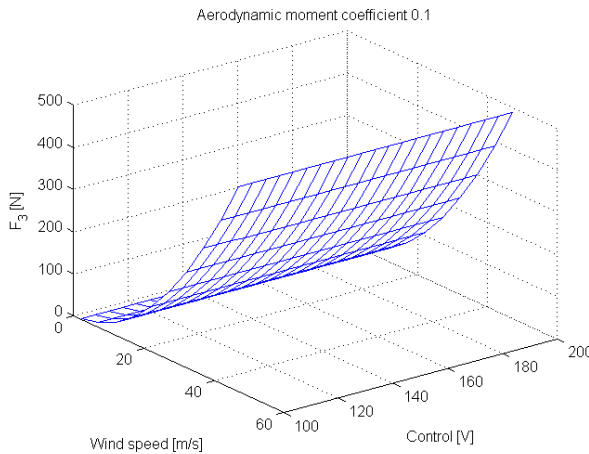
Fig. 12. Stationary values of the force F_3, developed by piezostack in the presence of the load F_a
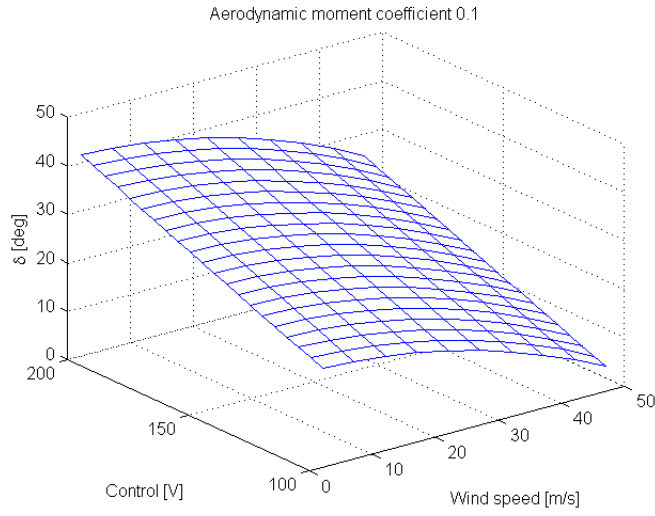
Fig. 13. Stationary values of the angle δ, developed by piezostack in the presence of the load F_a
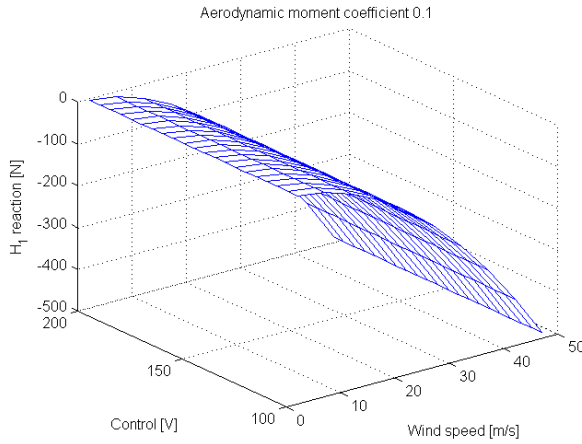
Fig. 14. Stationary values of the force H_1
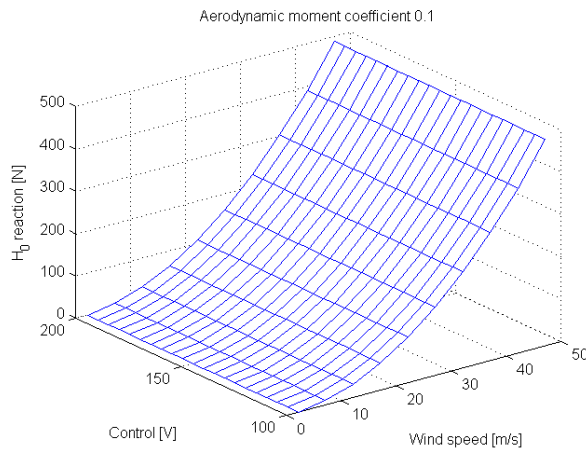
Fig. 15. Stationary values of the force H_0
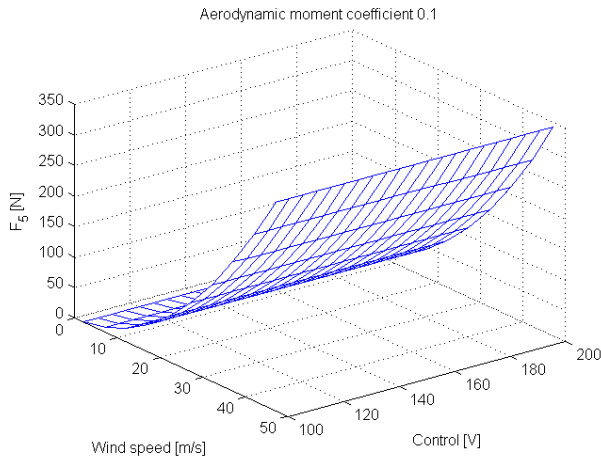
Fig. 16. Stationary values of the force F_5
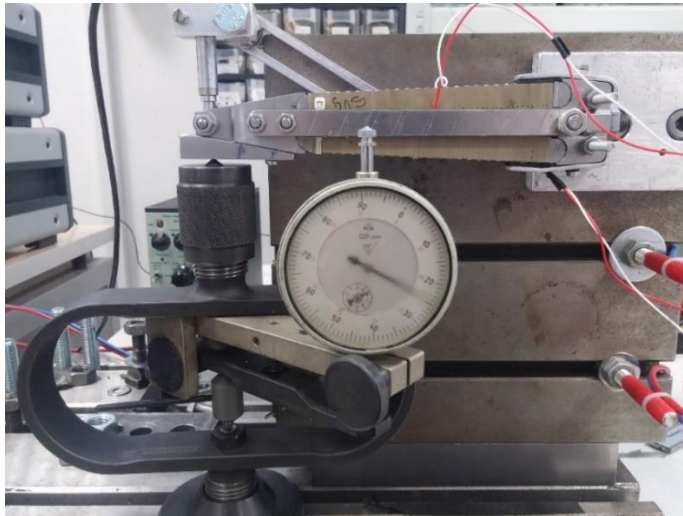
Fig. 17. V-piezo stacks actuator on measurements bench

A piezo actuator photo on measurements bench of INCAS Mechatronics Laboratory is shown in Fig. 17. This Laboratory has a tradition of over 45 years in analysis, synthesis, qualification testing and flight clearance for aircraft and helicopters hydraulic servomechanisms [10]-[19]. More recent is research on smart structures [20]-[23].

It is important to note that mathematical modeling presented in this article is original. The results prove that V-piezo stacks design has been well thought out. Further research must develop synthesis of antiflutter control law.

ACKNOWLEDGEMENTS

REFERENCES

[1] J. R. Newsom, and I. Abel, Active control of aeroelastic response, *NASA TM-83179*, July, 1981.

[2] J. Ko, A. J. Kurdilla, T. W. Strganac, Nonlinear dynamics and control for a structurally nonlinear aeroelastic system. *Department of Aerospace Engineering, Texas A&M University*, *TX 77843-3141*, 1997.

[3] I. Ursu, M. Stoia-Djeska, F. Ursu, Active control laws for flutter suppression, *Annales of University of Craiova, Electrical Engineering Series*, vol. **27,** no. 27, pp. 62-70, 2004.

[4] H. Ashley, S. M. Rock, R. Digumarthi, K. Chaney, A. J. Jr. Eggers, Active control for fin buffet alleviation, *WL-TR-93-3099*, January 1994.

[5] I. Ursu, F. Ursu, *Active and semiactive control* (in Romanian), Publishing House of the Romanian Academy, 2002, ISBN 973-27-0894-8.

[6] J. L. Pinkerton, A.-M. R. McGowan, R. W. Moses, R. C. Scott, J. Heeg, Controlled aeroelastic response and airfoil shaping using adaptive materials and integrated systems, *SPIE's 1996 Symposium on Smart Structures and Integrated Systems*, February 26-29, 1996, San Diego, CA.

[7] * * * Design of the wing. Piezoelectric actuator design. AFDPA system: manufacturing, implementation, static testing, INCAS Internal Report 15 031 C/2015, Phase 2, Contract 289/2014, December 2015.

[8] * * * *Antiflutter demonstrator with piezoelectric actuator*, PN-II-PT-PCCA-2013-4-2006, Contract 289/2014.

[9] E. V. Ardelean M. A. McEver, D. G. Cole, and R. L. Clark, Active Flutter Control with a V-Stack Piezoelectric Aileron Actuator, *Journal of Aircraft*, vol. **43**, no. 2, March–April 2006, pp. 482-486, 2006.

[10] I. Ursu, A. Toader, S. Balea and A. Halanay, New stabilization and tracking control laws for electrohydraulic servomechanisms, *European Journal of Control,* **19**, 1, pp. 65-80, 2013.

[11] I. Ursu, I., G. Tecuceanu, A. Toader, C. Calinoiu, Switching neuro-fuzzy control with antisaturating logic. Experimental results for hydrostatic servoactuators*, Proceedings of the Romanian Academy, Series A, Mathematics, Physics, Technical Sciences, Information Science*, **12**, 3, 231-238, 2011.

[12] A. Halanay, I. Ursu, Stability of equilibria of some switched nonlinear systems with applications to control synthesis for electrohydraulic servomechanisms, *IMA Journal of Applied Mathematics*, **74**, 3, June, 361-373, 2009.

[13] A. Halanay, C. A. Safta, F. Ursu and I. Ursu, Stability analysis for a nonlinear model of a hydraulic servomechanism in a servoelastic framework, *Nonlinear Analysis: Real World Applications*, **10**, 2, April, 1197-1209, 2009.

[14] I. Ursu, F. Ursu, F. Popescu, Backstepping design for controlling electrohydraulic servos, *Journal of The Franklin Institute*, USA, **343**, January, 94-110, 2006.

[15] A. Halanay, C. A. Safta, I. Ursu, F. Ursu (2004), Stability of equilibria in a four-dimensional nonlinear model of a hydraulic servomechanism, *Journal of Engineering Mathematics*, **49**, 4, August, 391-405, 2004.

[16] I. Ursu, F. Ursu, L. Iorga, Neuro-fuzzy synthesis of flight controls electrohydraulic servo. *Aircraft Engineering and Aerospace Technology*, **73**, pp. 465-471, 2001.

[17] I. Ursu, F. Ursu, T. Sireteanu, About absolute stable synthesis of electrohydraulic servo*, AIAA Guidance, Navigation, and Control Conference*, **1-3**, 848-858, Paper AIAA-99-4090, 1999.

[18] I. Ursu, G. Tecuceanu, F. Ursu, M. Vladimirescu, T. Sireteanu (1998), From robust control to antiwindup compensation of electrohydraulic servo actuators, *Aircraft Engineering and Aerospace Technology*, **70**, 4, 259-264, 1998.

[19] I. Ursu, Study of the stability and compatibility of hydraulic servo actuating flight controls, *INCAS Internal Report,* code 34125/ 20.12.1974, archive nr. 528.

[20] L. Iorga, H. Baruh, I. Ursu, A review of H_∞ robust control of piezoelectric smart structures, *Transactions of the ASME*, *Applied Mechanics Reviews*, **61**, 4, July, 17-31, 2008.

[21] E. Munteanu, I. Ursu, A. Alecu, Piezo smart wing with sliding mode control*, International Journal of Computers Communications & Control*, **3**, 417-421, 2008.

[22] L. Iorga, H. Baruh, I. Ursu, H_∞ control with μ-analysis of a piezoelectric actuated plate, *Journal of Vibration and Control*, **15**, 8, August, 1143-1171, 2009.

[23] I. Ursu, L. Iorga, A. Toader**,** G. Tecuceanu, Active Robust Control of a Smart Plate, *ICINCO 2011 8th International Conference on Informatics in Control, Automation and Robotics*, Noordwijkerhout, The Netherlands, 28-31 July 2011, Papers Compilation, pp. 27-36.